Clinical Neurophysiology 121 (2010) 2035–2043

Contents lists available at ScienceDirect

Clinical Neurophysiology

journal homepage: www.elsevier.com/locate/clinph

Reduced functional connectivity in visual evoked potentials in children with autism spectrum disorder

J.R. Isler [a,*], K.M. Martien [b,d], P.G. Grieve [a], R.I. Stark [a], M.R. Herbert [c,d]

[a] Department of Pediatrics, Columbia University, 630 W. 168th St., New York, NY 10032, USA
[b] Lurie Family Autism Center-LADDERS Clinic, Department of Pediatrics, Massachusetts General Hospital, Boston, MA, USA
[c] Department of Neurology, Massachusetts General Hospital, Boston, MA, USA
[d] TRANSCEND Research Program, Massachusetts General Hospital, Boston, MA, USA

ARTICLE INFO

Article history:
Accepted 6 May 2010
Available online 4 June 2010

Keywords:
Autism
Coherence
EEG
Power
Synchrony
Connectivity

ABSTRACT

Objective: An analysis of EEG synchrony between homologous early visual areas tested the hypothesis that interhemispheric functional connectivity during visual stimulation is reduced in children with autism compared to controls.
Methods: EEG power and coherence within and between two homologous regions of the occipital cortex were measured during long latency flash visual evoked potentials. Measures were compared between two groups of children (5.5–8.5 years), one with autism spectrum disorders and the other with typical development.
Results: In and below the theta band, interhemispheric synchrony was reduced in autistic subjects compared to typical controls by as much as 50%. Above the theta band interhemispheric synchrony in autistic children became indistinguishable from what would occur for uncorrelated cortical activity. Interhemispheric synchrony in autistic subjects was decreased in spite of bilaterally increased power. Wavelet power showed autistic children had a more rapid initial response to stimulation, a slower recovery, and more modulation at longer latencies.
Conclusions: Results suggest that the sensory cortices of autistic children are hypersensitive to stimulation with concurrent diminished functional connectivity between hemispheres.
Significance: Simultaneously increased intrahemispheric power and decreased interhemispheric synchronization of elemental visual information suggests either that power increases cause poor interhemispheric connectivity or that processes, such as thalamocortical regulation, impact power and coherence independently.

1. Introduction

Theories of autism spectrum disorders (ASD) propose that affected persons have diminished capacity for integration of brain activity because locally specialized cortical regions are less anatomically and/or functionally connected (Belmonte et al., 2004; Just et al., 2007). Anatomical studies have shown brain volume and white matter increases more frequently in younger than older subjects (Courchesne et al., 2001; Herbert et al., 2003; Herbert et al., 2004; Amaral et al., 2008), suggesting that these anatomical findings may not be directly implicated in function, since neuropsychological findings putatively attributable to connectivity do not vary in the same manner. In contrast, functional connectivity studies more consistently show decreases in subjects with ASD (Just et al., 2004, 2007; Villalobos et al., 2005; Cherkassky et al., 2006; Coben et al., 2008), though results are mixed (Murias et al., 2007).

An alternative, perhaps complementary, view is that inadequate integration is not solely based on a deficit in connectivity, but is also the consequence of sensory hypersensitivity. Elevated response to stimulation in sensory areas may overwhelm the capacity for effective communication further downstream within the brain (Belmonte and Yurgelun-Todd, 2003; Happe and Frith, 2006). Of interest this form of disconnection might yield richly detailed sensory processing capacities, perhaps accounting for perceptual advantages and savant skills (Gomot et al., 2008; Mottron et al., 2009).

Electroencephalography (EEG) provides windows into both proposed modes of disconnection. EEG power at a single electrode

* Corresponding author. Address: Department of Pediatrics, College of Physicians and Surgeons, Columbia University, P&S 3-440, 630 W. 168th St., New York, NY 10032, USA. Tel.: +1 212 342 4151; fax: +1 212 305 0956.
E-mail address: jri2101@columbia.edu (J.R. Isler).

1388-2457/$36.00
doi:10.1016/j.clinph.2010.05.004

reflects the degree of locally synchronous cortical activation (i.e. an increase in spectral power, analogous to but inherently better time-locked than "activation" in fMRI). EEG coherence is a bivariate measure of the degree of oscillatory synchrony (phase locking) between two brain regions and provides a measure of electrocortical functional connectivity (Nunez et al., 1997; Sporns et al., 2000).

Generally, synchronization of electric field potential oscillations is an efficient mechanism for coalescing local and regional assemblies into more widespread networks (Varela et al., 2001). Oscillatory synchrony is associated with cognitive functions including perception (Gray et al., 1989; Tallon-Baudry et al., 1996), attention (Buschman and Miller, 2007; Lakatos et al., 2008), memory (Sederberg et al., 2003), awareness (Rodriguez et al., 1999), and behavior control (Pfurtscheller et al., 1994; von Stein et al., 2000). In each of the traditional EEG frequency bands (delta 1–4 Hz, theta 4–8 Hz, alpha 8–12 Hz, beta 12–25 Hz, gamma > 25 Hz), synchrony facilitates distinct cognitive functions (Buzsaki and Draguhn, 2004; Buschman and Miller, 2007).

Interhemispheric synchrony between homologous sensory and motor areas provides an inherent mechanism for coordinating bilateral sensory and motor processing. For example, interhemispheric synchrony in the alpha band is correlated with object recognition (Mima et al., 2001) while in the beta band interhemispheric synchrony is associated with bilateral movement coordination (Nikouline et al., 2001).

Here, we tested the hypothesis that sensory specific functional connectivity is reduced in children with ASD. To that end, we evaluated interhemispheric synchrony between homologous early visual areas during visual stimulation. We also investigated the activation of sensory cortex in the same subjects by evaluating differences in EEG power in early visual regions.

2. Materials and methods

2.1. Participants

Twenty subjects between the ages of 5.5 and 8.5 years of age were recruited for this study: nine children with a clinical diagnosis of an ASD and eleven typically developing children. Legal guardians provided informed consent and competent subjects provided verbal assent in accord with the Institutional Review Board at Massachusetts General Hospital in Boston. Fourteen of the twenty participants provided adequate artifact-free long latency visual evoked potential (VEP) data for analysis. Of the participants whose data was excluded, three were autistic and three typically developing. The final cohort (see Table 1) was composed of individuals meeting full diagnostic criteria for autism ($n = 4$), individuals meeting criteria for an ASD ($n = 2$) and typically developing controls ($n = 8$).

Clinical impression of either an ASD or typical development on screening at the time of recruitment was required for initial inclusion. Diagnosis of an ASD was confirmed using the Autism Diagnostic Interview – Revised [ADI-R WPS] (Lord et al., 1994) and the Autism Diagnostic Observation Schedule [ADOS WPS] (Lord et al., 2000) (see Table 1). Diagnostic impression of an ASD was formally established after careful consideration of ADI-R and ADOS scores, in combination with expert clinical judgment that each subject met ASD criteria as set out in the Diagnostic and Statistical Manual of Mental Disorders, Fourth Edition (Association, 1994). In the two cases where full ADI/ADOS criteria of autism was not met, a diagnosis of an ASD was made based on meeting autism criteria on 2 of 3 domains on ADI-R and meeting 'ASD' criteria on the ADOS. Participants were excluded if, on review of medical history, any of the following conditions were identified: premature birth before 35 weeks, hypoxic/ischemic event at any point during development, sensorimotor deficit; known presence of structural brain lesion, major genetic or syndromic disorder; uncontrolled seizures or clinical evidence of progressive encephalopathy. Typically developing control candidates were included after screening out medical conditions affecting normal development and/or indications of developmental disability, psychiatric, or neurological disorder. This screening was performed utilizing parent questionnaires including Social Communication Questionnaire [WPS] (Berument et al., 1999), the Behavioral Assessment System for Children [BASC-2](Pearson Education, 2008) (see Table 2), and a medical history questionnaire. Additionally, all subjects were required to have English as the primary language spoken in the home.

For data analysis purposes, the ASD group was defined as all those children with autism or an ASD. The ASD group ($n = 6$) and typical group ($n = 8$) differed in mean age by one year (M age ASD group = 7.8 years, SD = 0.57, range 6.7–8.3; M age typical group = 6.8 years, SD = 0.76. range 5.9–8.0). Male to female ratio for the autistic sample was 5:1 (consistent with reported prevalence by gender), and for the typical group was 1:1. IQ was estimated using the Differential Abilities Scale [DAS] (Pearson) which generates a General Conceptual Ability (GCA) as well as verbal, non-verbal and spatial reasoning abilities (see Table 1). The groups differed significantly on GCA SS (ASD group $M = 67.83$, SD = 27.15, SS Range = 43–105; typical group $M = 117.13$, SD = 9.75, SS Range = 106–134). Among the six children in the ASD group, one had a diagnosis of epilepsy which was controlled by two antiepileptic drugs (AED): valproate (Depakote) and topiramate (Topamax), and took the nutritional supplement carnitine (Carnitor); one was on an AED, valproate, for an abnormal EEG without evidence of clinical seizures; one was reported to have an abnormal EEG with unilateral slowing and no history of seizures; one was being treated with an SSRI (fluvoxamine) for anxiety. Two participants, one autistic and one typical, were treated with anti-inflammatory/cytokine modulating agents: one (autistic) was on montelukast (Singulair) for food allergies and one (control) was on sulfasalizine (Azulfidine) for inflammatory bowel disease. One additional control was on fexofenadine (Allegra) for environmental allergies.

The Dunn Sensory Profile (Dunn, 1999) parent questionnaire was used to determine atypicality of sensory system functioning. All children with ASD had numerous sensory differences on the profile varying by subject but including domains of: sensory

Table 1
Autistic subjects.

Subject	Gender	Age	Clinical Dx	ADOS/ADI-R classification	DAS–GCA	Seizure history?
1	M	6.7	Autism	Autism/autism	43	No
2	F	7.8	ASD	ASD/autism	92	No
3	M	7.8	Autism	Autism/autism	53	No
4	M	8.1	ASD	Autism/ASD*	39	Yes
5	M	8.1	Autism	Autism/autism	105	No
6	M	8.3	Autism	Autism/autism	75	No

* Met criteria for autism on social and communication, not repetitive behavior.

Table 2
Control subjects.

Subject	Gender	Age	SCQ classification	BASC-2 sign. domains	DAS–GCA
1	F	5.9	No ASD	None	106
2	M	6.2	No ASD	None	106
3	F	6.2	No ASD	None	125
4	F	6.3	No ASD	None	119
5	M	6.6	No ASD	None	113
6	F	7.3	No ASD	None	134
7	M	7.6	No ASD	None	122
8	M	8.0	No ASD	None	112

processing 5/6, modulation 5/6, and behavioral/emotional responses 4/6. None of the typically developing subjects had significant atypicality in sensory processing, modulation or behavioral/emotional responses.

2.2. Protocol, recording, pre-processing

EEG and ERPs were recorded in an acoustically and electrically shielded room. A long latency flash visual evoked potential (VEP) paradigm was used to achieve activation of early (low level) visual cortex. White light stroboscopic flashes were delivered approximately 1 m from the eyes at a luminance of $\sim$ 1.375 lumen sec/ft^2 (setting 1 on a Grass PS33plus photic stimulator). The intertrial interval was 1.05 s. Flashes were delivered in 1 block of $\sim$ 64 flashes. EEG data were recorded with an Electrical Geodesics Inc. (EGI) system using 128 electrode nets (Hydrocel Geodesic Sensor Net soaked in KCl solution) fitted to the head and allowing no more than 50 k ohm impedance at any given electrode. Electrodes were referenced to Cz during recording (subsequent analysis used average reference). Data were sampled at 1000 Hz and hardware filtered during recording below 400 Hz and above 0.1 Hz.

After recording, a 1600 point linear phase software notch filter (4 Hz wide notches with 60 dB falloff within 2 Hz of the notch edges) for 60 Hz and its harmonics up to 360 Hz was applied to the data. Recordings were segmented into trials of 1 s length (100 ms pre-stimulus). Head movement and other artifact were detected automatically for each trial and channels were rejected for a trial if any of the following criteria were met: absolute sample-to-sample change greater than 25 μV; absolute value greater than 600 μV; standard deviation greater than 50 μV; and spectral slope between 20 and 200 Hz greater than −0.1 (to detect muscle artifact). Trials with more than 25% of channels matching one of the above criteria were rejected. For the remaining trials, eye movements were detected and rejected visually on a trial-by-trial inspection using a bipolar montage of smoothed (40-point boxcar) raw data from eleven channels near the eyes as well as inspection of the full 128 channel montage for spatial patterns suggesting eye movements. We were extremely conservative in this regard, removing trials even with only weak evidence of eye movements. Finally, data were re-referenced to the average reference of artifact-free channels for all subsequent analyses. All analyses were performed using the Matlab programming language.

Flash VEP has a high signal to noise ratio and can be measured with a relatively small number of trials (Brigell et al., 1998). Of an original cohort of 20 (5.5–8 years) subjects, those with fewer than 18 artifact-free trials remaining were excluded from further analysis. The mean number of trials in the autistic group was 31 and in the control group 37 (statistical biases were corrected; see below). The primary reason for exclusion of other subjects from the study was the presence of trials with eye movements.

For this study two regions of interest (ROI) over left and right early visual areas were defined (Fig. 1). For left and right ROI estimates of power, the mean of natural log power was taken over the six neighboring ipsilateral electrodes in each ROI. For interhemispheric synchrony, the mean of all 36 interhemispheric pairs was used after correcting for volume conduction bias (see below). Group differences were subsequently taken across these within-subject means.

2.3. Data analysis

Fast Fourier transforms (FFTs) were computed for each 1 s trial after removal of the mean and application of a Hann window. *Power spectra* were calculated as the magnitude-squared FFTs averaged across trials (the numerator of Eq. (1) with $i = j$). Cross spectra were calculated by averaging the product of one channel FFT with the complex conjugate FFT of another channel for all possible pairs (i,j) of channels across trials; *coherence*, $C_{ij}(f)$, was calculated as the magnitude of the cross spectrum normalized by the square root of the product of the channel powers (Bendat and Piersol, 2000)

$$C_{ij}(f) = |\langle X_i(f)X_j^*(f)\rangle|/[\langle|X_i(f)|^2\rangle\langle|X_j(f)|^2\rangle]^{1/2} \quad (1)$$

where $X_i(f)$ and $X_j(f)$ were the frequency (f)-dependent complex Fourier transforms of the two time (t) series $x_i(t)$ and $x_j(t)$ and the brackets represent an average across trials. To address temporal evolution of post-stimulus power, we computed *wavelet power* with a mother Morlet wavelet of four cycles at 10 scales per octave, ignoring time–frequency regions susceptible to edge effects. Wavelet power was computed using programs modified from (Torrence and Compo, 1998).

Phase synchrony between pairs of electrodes was measured as 1 minus the circular variance across trials of the difference between FFT phases

$$PS_{ij}(f) = |\ \langle \exp[i(\phi_i(f) - \phi_j(f))]\rangle\ | \quad (2)$$

where ϕ_i and ϕ_j were the phases of the Fourier transforms X_i and X_j. Whether coherence or phase synchrony is the preferred mea-

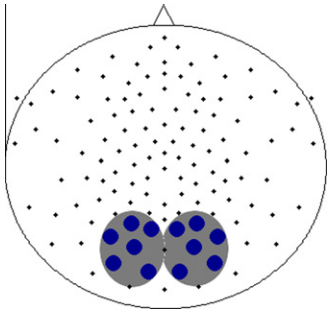

Fig. 1. The two (left and right) regions of interest (ROI) are denoted by blue shaded electrode locations projected onto a plane with all other electrode locations (nose at the top). Two ROI, each containing six electrodes, were defined over the left and right occipital areas, respectively (O1 and O2 in the international 10–20 system are the middle electrodes on each side). (For interpretation of the references to colour in this figure legend, the reader is referred to the web version of this article.)

sure of synchrony remains a subject of some debate (Nolte et al., 2004); each may be susceptible to its own subtle forms of "algorithmic" artifact. For these reasons, to quantify synchrony we calculated both quantities. Coherence has a statistical bias that is proportional to $N^{-1/2}$, where N is the number of trials, but that also depends on the "true" value of the quantity being computed (Carter et al., 1973). Since the latter is unknown and the N's in this study were not large, we chose to exploit our system's amplifier noise in order to estimate statistical bias. Since a low-pass hardware filter at 400 Hz was applied during recording and the sampling rate is 1000 Hz, spectral quantities near the Nyquist frequency of 500 Hz should only reflect properties of the amplifier noise, because physiological signals have been filtered out at those frequencies. Assuming that amplifier noise is random and uncorrelated across electrode channels, an estimate of maximal statistical bias for the case of zero synchrony can be calculated as the mean of values near 500 Hz (we used 480–499 Hz). This estimate was then removed on a per subject basis, since there were variable numbers of trials across subjects, prior to group analysis. Prior to this procedure, each subject's coherence and phase synchrony reached an asymptotically flat, non-zero value at the highest frequencies, but at a level that varied across subjects. After this procedure, all the subjects had approximately the same non-zero value at the highest frequencies (due to residual volume conduction bias, discussed next).

Both synchrony measures (coherence and phase synchrony) for nearby electrodes are biased by volume conduction, to a degree that varies as a function of inter-electrode distance (see Discussion). As a consequence, coherence (or phase synchrony) averaged over pairs of electrodes is biased towards the physically closer pairs. However, Nunez et al. (1997) suggested a procedure to remove the effects of volume conduction, using the formula $\exp[(1-x)/a]$, where x is inter-electrode distance on the scalp and a is a scale factor. The procedure is to estimate volume conduction bias for each pair of electrodes, subtract it from the measured coherence, and set it to zero if it becomes negative. The resulting quantity, *reduced coherence*, estimates the true physiological synchronization of oscillations between two sites. Because coherence is a nonlinear quantity, the simple subtraction used in reduced coherence makes it a first order estimate of true physiological synchrony. We used the above formula with $a = 3.73$ cm for this study (corresponding to a 4 cm scale factor on the adult head (Nunez et al., 1997)) and with x calculated for a head radius of 8.4 cm (mean measured head circumferences were 54.5 cm in the ASD group and 52.7 cm in the control group). We then subtracted the estimated bias from the computed coherence and phase synchrony for each electrode pair between the two ROI.

Subsequently, group statistics (mean, standard error) were calculated for differences and t-tests were used to determine significance for each quantity, i.e. power, wavelet power, coherence, and phase synchrony. Repeated measures analysis of variance (ANOVA) was applied to log wavelet power at each frequency.

3. Results

Our results show that autistic children had less interhemispheric synchrony between early visual areas than controls, in spite of greater intrahemispheric power than controls. Fig. 2 shows power spectra averaged within the two ROI (left and right occipital areas) for the autistic and control groups from 1 to 300 Hz. Mean power in both ROI was greater in the autistic group than in the control group over a broad range of frequencies. Significantly increased power in the autistic group occurred bilaterally at 4 Hz and in both the alpha and lower beta bands (10–15 Hz), but only on the right in the upper beta band (16–23 Hz). Spectral power trended higher in the autistic group up to frequencies as high as 100–150 Hz. Note the spectral peak in the autistic group in the alpha band not present in the control group.

Fig. 3 shows time–frequency plots of wavelet power and regions with significant differences across groups. As it should, the time-averaged wavelet spectrum agrees with the results in Fig. 2, namely increased power in both ROI in the autistic group over a wide range of frequencies; however, the full wavelet result reveals several features of the post-stimulus evolution of power. First, the response at early latencies (<200 ms) in the upper theta, alpha, and beta bands is significantly larger in autistic subjects and has a broader time–frequency peak. Second, in both ROI, theta/alpha power peaks much earlier in the autistic group, especially on the right, where the peak occurs nearly twice as rapidly. Specifically, alpha power peaks at ~90 ms on the right and ~120 ms on the left in the ASD group, compared to ~160 ms on the right and ~170 ms on the left in the control group. Third, compared to control subjects, the decay of power at longer latencies is less uniform in the ASD subjects. Inspection of the middle panel of Fig. 3 shows that at later time points power in the alpha and beta bands shows greater post-stimulus modulation in ASD subjects than in controls. These modulations account for the significant group differences at longer latencies (e.g. at about 400 ms on the right).

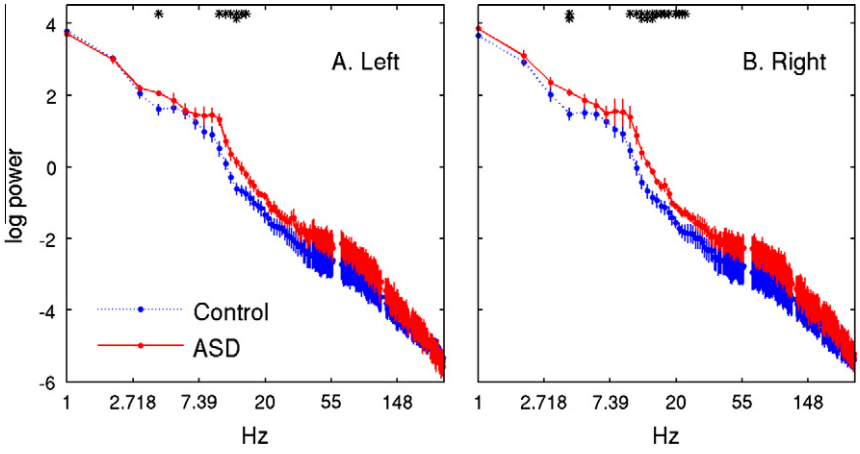

Fig. 2. Group mean natural log power within the left (A) and right (B) ROI (see Fig. 1 for locations). Autistic group is denoted by red solid curve, control group by blue dotted curve. Errors bars denote standard error. Single (double) asterisks denote frequencies with significant ($^{*}p < .05$, $^{**}p < .01$) differences between groups. This measure of local activation includes a peak in the alpha band in autistic subjects not seen in control subjects.

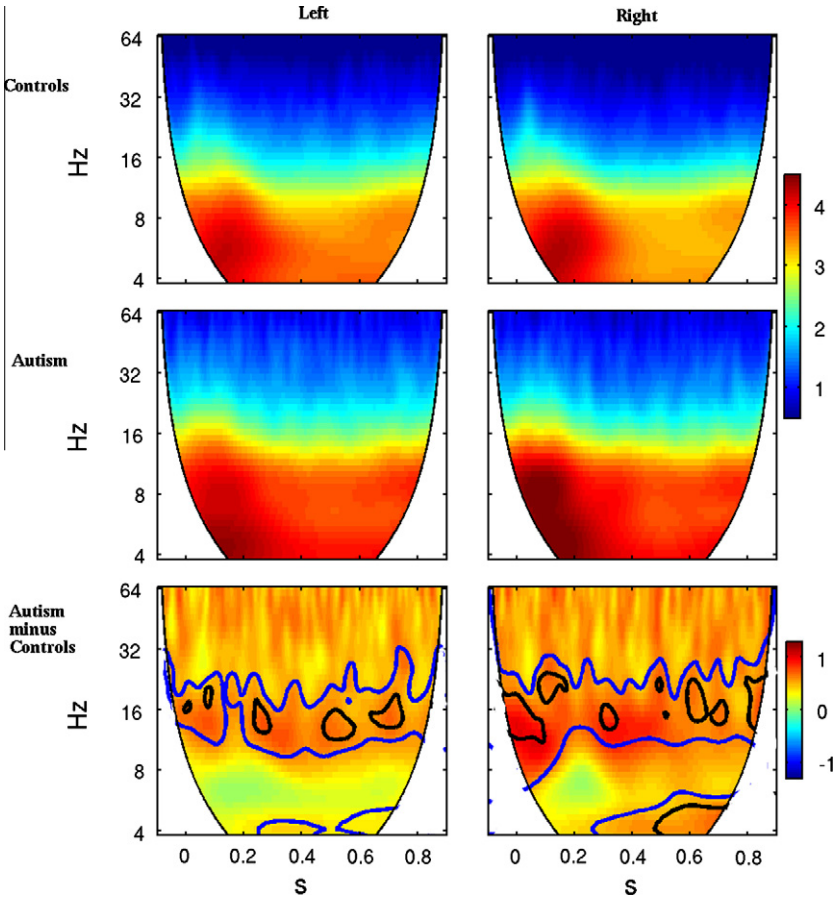

Fig. 3. Control and autistic subjects log wavelet power in the left and right ROI. Visual flash is at $t = 0$. Time–frequency regions unresolved by the 1 s window are obscured by white shading. Bottom: values of autistic minus control subject log wavelet power. Contour lines show time–frequency regions where the difference is significant ($p < .05$ within blue line, $p < .01$ within black line). Wavelet power trended higher in the autistic group across all frequencies excluding 4–8 Hz (compare Fig. 2). The autistic group had a stronger, more rapid and persistent response to the stimulus in the theta, alpha and beta bands. Repeated measures ANOVA indicated significant group by time interactions in the right ROI from 4 to 11 Hz.

Repeated measures analyses of variance of wavelet power in the two groups were carried out using group as a between subjects variable and time points (values for each ms) as the repeated, i.e. within subjects, measures. Separate analyses were conducted for each frequency and ROI. The main effect for time was highly significant ($p < .001$) for all frequencies in both ROI. The main effect for group was significant in both ROI from 10 to 20 Hz (to 24 Hz on the right) and in the right ROI from 4 to 5 Hz. Interestingly, significant group by time interactions were found for all frequencies from 4 to 11 Hz, but *only in the right ROI*. At the upper end of this range, from 7 to 11 Hz, the group by time interaction was driven by peak power occurring ~70 ms earlier in the autistic compared to the control group (90 ms versus 160 ms). At the lower frequencies of this range, from 4 to 6 Hz, the group by time interaction was driven by both a slower falloff from peak power and a tendency for power to rise again after ~500 ms in the ASD group.

Fig. 4 shows spectra of two measures (coherence and phase synchrony) that quantify the degree of interhemispheric synchrony between the two homologous ROI. Both measures are normalized quantities with 0 denoting uncorrelated signals and 1 denoting perfectly synchronized signals (with or without a lag in time). The frequency axis is shown in log format from 1 to 300 Hz as in Fig. 2. Both coherence (top) and phase synchrony (bottom) have similar features for both groups of children.

For both phase synchrony and coherence and across both groups of children, the largest interhemispheric values occur at low frequencies in the delta and theta bands. Above these bands, the degree of synchrony fell to a level of about 0.1 and maintained this level out to the highest frequencies. However, there were numerous differences between the two groups in both measures. In general, *autistic subjects had less* interhemispheric *synchrony than controls, in spite of having greater power than controls in each hemisphere separately*. At and below the theta band, interhemispheric synchrony was reduced in the autistic group by as much as 50%. Significant reductions occur at 2, 3, 5, 6, 8, 9, 10, 12–29 and 44 Hz for coherence and at 2, 5, 10, 14, 16–19, 22–24 and 27–30 Hz for phase synchrony. Strikingly, across the theta band of the autistic group interhemispheric synchrony fell precipitously and by 9 Hz reached a high-frequency asymptotic value (likely due to volume conduction; see below) for both coherence (top) and phase synchrony (bottom). In stark contrast, in the control group both measures of synchrony fell off much more gradually and reached an asymptotic value above ~80 Hz. These differences in the rapidity with which synchrony decays to an asymptotic value were the reason for the significant reductions of interhemispheric synchrony in autistic compared to control subjects at numerous frequencies in the alpha, beta and low gamma bands.

Fig. 4 shows frequencies (with asterisks) where group means were significantly different from each other. We also applied significance tests within each group, testing whether the group mean was significantly different from the asymptotic high-frequency level (computed as the mean from 100 to 300 Hz). Results showed that coherence and phase synchrony in the ASD group were not significantly above the high-frequency asymptote for any frequency

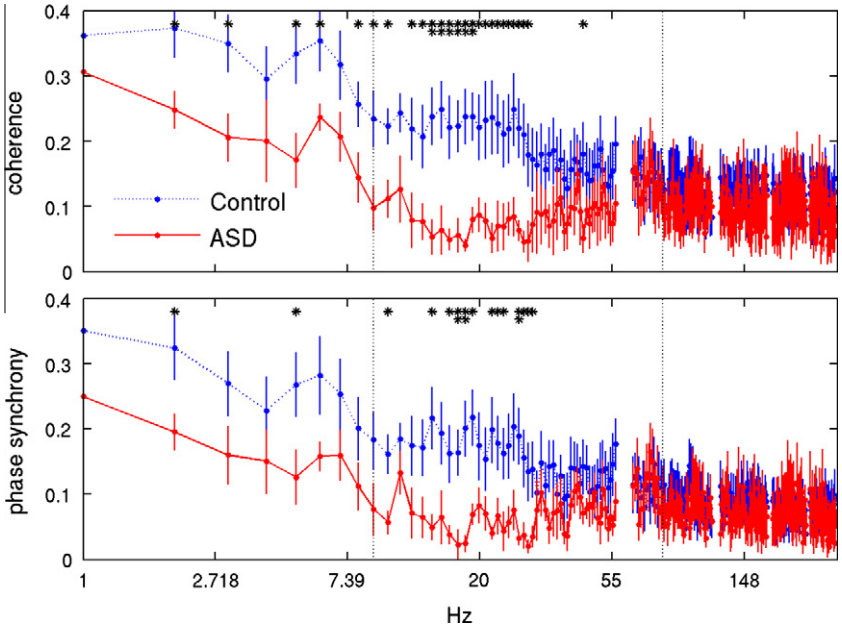

Fig. 4. Interhemispheric synchrony between left and right ROI as measured by coherence (top) and phase synchrony (bottom) spectra. Autistic group is denoted by solid red curve, control group by dotted blue curve. Errors bars denote standard error. To aid discussion in the text, vertical lines are drawn at 9 and 80 Hz. Group differences are significant at $^{*}p < .05$, $^{**}p < .01$.

above 7 Hz, while for the control group significance was maintained up to 30 Hz. The ASD group size is small ($n = 6$), so to address what fraction of ASD subjects were at or below the asymptotic level at frequencies above 9 Hz, we pooled results across subjects and frequencies from 10 to 20 Hz and found that 70% were below the high-frequency asymptote in the ASD group, compared to 15% in the control group.

4. Discussion

The primary goal of this study was to test the hypothesis that wide-area functional connectivity in a stimulated state is reduced in children with autism compared to typically developing children. To this end, we evaluated interhemispheric functional connectivity between left and right early visual areas in response to light flash stimulation with computation of both coherence and phase synchrony. We found that both measures in fact discerned a reduction of interhemispheric synchrony in autistic subjects. Surprisingly, besides being reduced at frequencies at and below the theta band, interhemispheric synchrony above the theta band was essentially the same as an asymptotic high-frequency level in the autistic subjects in our study (see below). A second goal of the study was to investigate the degree of elevated sensory activation in autism. To that end we evaluated EEG power separately within left and right occipital regions as a measure of local activation of early visual cortex. In agreement with previous studies, we found increased sensory activation in autistic subjects. The number of subjects in the final cohort was quite small, so there is the possibility that results were driven by just a few subjects. However, where significant differences were found, there was generally little overlap between the two groups. For example, in Fig. 4 from 10 to 25 Hz the overlap between the two groups was two subjects or less at all frequencies where significance was found.

4.1. Power

Group differences in EEG power can be confounded by different levels of artifact, so first we discuss how we controlled for that. To eliminate eye movement artifact, we removed all trials with blinks prior to analysis, as described in Section 2. Recently, however, it was reported that even very small eye motions (microsaccades) generate scalp EEG power in the gamma and higher bands that can easily be mistaken for cortical activation in those bands (Yuval-Greenberg et al., 2008). To test whether our results were contaminated by microsaccades, we looked at high-frequency power over all electrodes, i.e. not just in the two ROI. The largest and most significant group differences occurred over the occipital region which is farthest from the eyes, providing strong evidence that the beta and low gamma band power differences between groups observed here are not due to microsaccades or other eye movements. Another source of artifact in EEG power is muscle activity. Muscle artifact most commonly arises from the temporalis muscles attached to parietal and frontal skull regions that control jaw movements. We cannot rule out the possibility that differential occipital (neck) muscle activity contributed to the group power differences.

Previous studies found increased local activation in early auditory (Gomot et al., 2008) and visual (Orekhova et al., 2007; Milne et al., 2009) processing in autism, though results are mixed (Lazarev et al., 2009). Our finding of increased EEG power in the visual ROI of autistic subjects extends the results from those studies in several ways. First, wavelet analysis revealed that theta/alpha power peaked much earlier in the autistic group, consistent with a similar finding by Milne et al. (2009) in a study of older (~12 years) autistic children. In our case, earlier theta/alpha power was most pronounced in the right occiput. Greater EEG power at lower latency suggests reduced inhibition in the thalamocortical circuitry of the early visual system in autism, and provides support to the hypothesis that reduced functional connectivity in autism may be due to hypersensitive sensory systems. Second, there was a spectral peak in alpha band power in autistic children that was absent in control children. A prominent peak in the alpha band has long been known to occur in adults when eyes are closed, i.e. during reduced stimulation of visual cortex. In contrast, for autistic children we found a peak in the alpha band *during visual stimulation*. This may represent a disturbance in the circuitry responsible

for generating the alpha rhythm. Perhaps this activity is due to a stimulus-induced resonant "ringing" of the alpha circuit in autistic children that is usually prevented by inhibition. Elevated occipital alpha power during visual stimulation was also noted by Milne et al. (2009), and appears to be consistent with findings reported by Lazarev et al. (2009) (in Fig. 1, in Lazarev et al. (2009), alpha power at occipital electrodes during visual stimulation was ~50% larger in the autistic subject in a comparison of representative subjects). Third, there was increased power bilaterally in the beta band that was shown by wavelet analysis to persist to longer times post stimulation in the autistic group.

It is important to note that because of the lack of a baseline period, increased power in the ASD group might be stimulus-independent, consistent with reduced alpha blocking in subjects with ASD (see "Baseline differences" below). For example, Coben et al. (2008) found elevated right posterior theta band power in autistic subjects in unstimulated conditions. However, the consistency of our findings with those of Milne et al. (2009), who used a baseline period, suggests that our finding is at least partially driven by the visual stimulus.

In short, the early visual areas of autistic children were hypersensitive to stimulation compared to controls with a stronger and more rapid initial response, a slower recovery, and more modulation than the same areas in the control group. The finding of hypersensitive early visual cortex, especially in the alpha band, may relate to fMRI findings of increased thalamocortical connectivity in autism (Mizuno et al., 2006). It could also be due to local alterations in cellular responsivity due to such factors as excitotoxicity related to glial cell activation (Pardo and Eberhart, 2007). The result also provides support for the idea that the "disconnection syndrome" of autism may be due to hypersensitive sensory areas (Belmonte and Yurgelun-Todd, 2003; Happe and Frith, 2006).

4.2. Interhemispheric synchrony

Group differences in synchrony can be confounded by group differences in power, so first we discuss this confound. Volume conduction contributes to measurements of synchrony because the potential field recorded at one location is a superposition of potentials from multiple sources that superimpose to some extent at nearby locations. Thus, a correlation between potentials from neighboring electrodes exists even when the neural activity immediately beneath the electrodes is not correlated. As a result, synchrony estimates for nearby electrodes are biased by volume conduction, to a degree that varies as a function of inter-electrode distance. One way to mitigate the effect of volume conduction is by taking spatial derivatives of the potential field at each electrode, usually either a first derivative (bipolar montage) or second derivative (surface Laplacian, or current source density), and then analyzing those quantities instead of the electric potentials. We did not do this (applying spatial derivatives further reduced group sizes, already small, because of more stringent good channel/trial requirements); rather, we report reduced coherence (see Section 2), which removes an estimate of volume conduction bias from raw coherence values. However, when (as in this study) group differences are of primary interest, volume conduction bias subtracts out and the need for other approaches is partially mitigated. Volume conduction effects would be completely removed if not for the fact that differences in power are a potential confound for differences in synchrony. Increased (or decreased) power at one location increases (or decreases) the contribution of volume conduction to the synchrony measured between that location and other locations. The important point to bear in mind is that power differences can confound synchrony differences *only if the differences in both cases have the same sign*. Since the autistic group in this study had reduced synchrony together with increased power, the synchrony reduction cannot be an artifact of volume conducted power differences.

4.3. Residual volume conduction bias

As mentioned above, in Fig. 4 in all cases (for both measures, from both groups) synchrony appears to achieve an asymptotic value at the highest frequencies, suggestive of a measurement bias remnant in the reduced quantities. The mean of the coherence spectra between 100 and 300 Hz is 0.10 and 0.11 for the autistic and control subjects, respectively. Similarly, the mean of the phase synchrony spectrum over the same range was smaller in autistic subjects compared to control subjects (0.07 versus 0.08). Since the head sizes of the autistic children were slightly larger than those of controls (mean circumference of 54.5 cm versus 52.7 cm), one would expect volume conduction bias to be slightly less in autistic compared to control subjects because the inter-electrode distances were slightly greater. Thus, the slightly smaller asymptotic mean value for both measures in autistic subjects supports its interpretation as a residual measurement bias, most likely due to volume conduction bias that was not completely removed by the approximate formula used for reduced quantities. This provides a new interpretation for Fig. 4 with respect to autism. If the asymptotic value of ~0.1 is due to residual volume conduction bias, then the autistic subjects have *interhemispheric synchronization above the theta band indistinguishable from what would occur for uncorrelated cortical sources*. In stark contrast, reduced synchrony in the control group does not become indistinguishable from the asymptotic value until 30 Hz, with values trending downward to 80 Hz.

As introduced earlier, synchronization of field potential oscillations between brain regions is an efficient mechanism for coalescing (connecting) regional assemblies into more widespread networks. Various theories have put forward the notion that deficits in connectivity are a primary causal factor of autism. In particular, it is supposed that widespread cortical areas do not function in as integrated a fashion as normally required for higher-order cognitive processes such as attention and memory. Our novel finding that autistic subjects have severely reduced functional connectivity between right and left visual areas in response to visual stimulus supports these theories. Previous studies of electrocortical synchrony in autism have found a mixture of increased and decreased coherence (Murias et al., 2007; Coben et al., 2008) but in these studies EEG was recorded in the eyes closed resting state rather than a stimulated state as in the present study. This suggests that the process of active sensory processing may exacerbate the connectivity deficits seen in autism. In a study that did include visual stimulation, Lazarev et al. (2010) looked at thresholded coherence during photic driving stimulation and found asymmetry in autistic boys that was not present in typically developing boys, with greater coherence in the left hemisphere. However, the authors note that within individuals coherence is well correlated with power at the driving frequencies, so their inferences regarding connectivity are confounded by power differences.

As noted in the Introduction, field potential oscillations in distinct frequency bands may subserve distinct cognitive functions (Buzsaki and Draguhn, 2004; Buschman and Miller, 2007). In this light, a salient feature of our findings, assuming the high-frequency asymptotic levels in Fig. 4 are due to residual volume conduction bias, is that interhemispheric synchrony is reduced above the theta band in autistic subjects to a level indistinguishable from what would occur due to uncorrelated cortical activity. In contrast, it fell off more gradually in control children, significantly to 30 Hz and trending downward to ~80 Hz. Within and below the theta band, interhemispheric synchrony was decreased by as much as 50% in the ASD group. Group sizes are not large in this study and results

will need to be confirmed in a larger study; but if these findings are true more globally in the brain (i.e. for more than just homologous visual areas), then these deficits could provide a causal mechanism for some of the features of autism. In fact, two predictions that follow directly from these results are that aspects of cognition subserved by wide-area synchrony at and below the theta band will be *reduced* in autistic subjects, while those aspects subserved by wide-area synchrony at frequencies above the theta band would be *absent* or accomplished, if at all, by alternate mechanisms. For example, interhemispheric synchrony in the alpha band between homologous visual areas has been correlated with object recognition for objects spanning the visual midline (Mima et al., 2001). Thus, the reduction in interhemispheric synchrony seen in the alpha band in this study suggests one potential source of impaired visual perception in autistic children.

4.4. Potential covariates

The two groups of subjects had variable age, antiepileptic drug (AED) use, and IQ (IQ variables were DAS standard composite scores; GCA, VC, NVC, SC and SNC). Univariate ANOVA indicated that none of these covariables significantly predicted occipital power or interhemispheric coherence for pooled group values. Given the limited total number of subjects ($n = 14$), a proper multivariate ANOVA even for two factors (group and one covariable) could not be performed. But it is interesting to note that none of the potential covariates was predictive of power or coherence for the pooled group.

4.5. Medication effects

Two of the autistic subjects were on antiepileptic drugs (AEDs), valproate ($n = 2$) and topiramate ($n = 1$), at the time of testing. EEG studies in epilepsy and VEP studies in bipolar disorder have found decreased amplitude/power after AED treatment, for valproate in particular (Clemens et al., 2006; Ozerdem et al., 2008). Thus, we do not believe that the findings of power differences are likely to be a result of AED effects, rather the differences might have been even greater if all the subjects had been AED drug naïve. The impact of AEDs on baseline or stimulated broad band coherence has not been well studied and therefore the impact of the AEDs on the coherence findings cannot be assessed. Other drugs (SSRIs and non-steroidal anti-inflammatory drugs) used by some subjects are unlikely to have impacted the findings, but there is essentially no literature on their effects in power or coherence.

4.6. "Baseline" differences

We made additional recordings EEG during a condition meant to expose group differences during "lack of stimulation". In this condition, children sat quietly in a dimly lit room with eyes open. We found nearly all the children with ASD did not tolerate the experience well and there was too much artifact in the EEG for subsequent analysis. For the visual flash experiment reported here, we analyzed Fourier coherence (Fig. 4, top), phase synchrony (Fig. 4, bottom) and spectral power (Fig. 2) over a 1 s interval for maximum frequency resolution. Therefore, there are no explicit pre- versus post-stimulus comparisons. However, as discussed above, wavelet power differences (Fig. 3, bottom) provide some insight. On the one hand, in the left ROI in the beta band differences are as large in the pre-stimulus period as afterwards, suggesting a relatively stimulus-independent effect, though it is equally possible that during stimulation "baseline" levels rise in the ASD group but not in the control group. On the other hand, in the right ROI in the alpha and theta bands there is clearly a time-dependent, low latency effect while in the beta band the largest differences are also at those times. Thus, in the right ROI for EEG power, there are group differences that are unambiguously stimulus-driven.

The findings reported here suggest that the sensory cortices of the autistic brain are hypersensitive to stimulation with poor functional connectivity to homologous cortex across hemispheres. Whether hypersensitivity undermines functional connectivity or is merely a co-existent phenomenon remains to be elucidated. But if this combination of properties occurs more generally in diverse areas of cortex, it could explain the fact that a savant's skills, which may depend upon relatively localized activation, can be dramatically above normal levels while co-occurring with profound deficits in cognitive functions that require wide-area connectivity. Finally, we suggest that the type of measures used in this study when applied to earlier periods in development will have the potential to provide diagnostic tools that can be used to define the risk of autism in infant and toddler populations, severity of neurobiological dysfunction and, hence, measures of treatment efficacy.

Acknowledgements

This work was supported by the National Institutes of Health [Grant No. NINDS 5K25NS052230], Cure Autism Now/Autism Speaks, the Nancy Lurie Marks Family Foundation, the National Alliance for Autism Research, and The Commonwealth Fund. The authors thank Professor Jerome Kagan of Harvard University, Dr. Charles Schroeder of Columbia University and the Nathan Kline Institute, and Dr. Michael Meyers and Dr. Amanda Tarullo of Columbia University for helpful comments.

References

Amaral DG, Schumann CM, Nordahl CW. Neuroanatomy of autism. Trends Neurosci 2008;31(3):137–45.
Association, AP. Diagnostic and Statistical Manual of Mental Disorders, 4th ed.; 1994.
Belmonte MK, Cook Jr EH, Anderson GM, Rubenstein JL, Greenough WT, Beckel-Mitchener A, et al. Autism as a disorder of neural information processing: directions for research and targets for therapy. Mol Psychiatry 2004;9(7):646–63.
Belmonte MK, Yurgelun-Todd DA. Functional anatomy of impaired selective attention and compensatory processing in autism. Brain Res Cogn Brain Res 2003;17(3):651–64.
Bendat JS, Piersol AG. Random data: analysis and measurement procedures. 3rd ed. New York: Wiley; 2000.
Berument SK, Rutter M, Lord C, Pickles A, Bailey A. Autism screening questionnaire: diagnostic validity. Br J Psychiatry 1999;175:444–51.
Brigell M, Bach M, Barber C, Kawasaki K, Kooilman A. Guidelines for calibration of stimulus and recording parameters used in clinical electrophysiology of vision. Doc Ophthalmol 1998;95:1–14.
Buschman TJ, Miller EK. Top-down versus bottom-up control of attention in the prefrontal and posterior parietal cortices. Science 2007;315(5820):1860–2.
Buzsaki G, Draguhn A. Neuronal oscillations in cortical networks. Science 2004;304(5679):1926–9.
Carter GC, Knapp CH, Nuttall AH. Statistics of estimate of magnitude-coherence function. IEEE Trans Acoust Speech 1973;21(4):388–9.
Cherkassky VL, Kana RK, Keller TA, Just MA. Functional connectivity in a baseline resting-state network in autism. Neuroreport 2006;17(16):1687–90.
Clemens B, Menes A, Piros P, Bessenyei M, Altmann A, Jerney J, et al. Quantitative EEG effects of carbamazepine, oxcarbazepine, valproate, lamotrigine, and possible clinical relevance of the findings. Epilepsy Res 2006;70(2–3):190–9.
Coben R, Clarke AR, Hudspeth W, Barry RJ. EEG power and coherence in autistic spectrum disorder. Clin Neurophysiol 2008;119(5):1002–9.
Courchesne E, Karns CM, Davis HR, Ziccardi R, Carper RA, Tigue ZD, et al. Unusual brain growth patterns in early life in patients with autistic disorder: an MRI study. Neurology 2001;57(2):245–54.
Dunn W. Sensory profile. Pearson educational; 1999.
Gomot M, Belmonte MK, Bullmore ET, Bernard FA, Baron-Cohen S. Brain hyper-reactivity to auditory novel targets in children with high-functioning autism. Brain 2008;131(Pt 9):2479–88.
Gray CM, Konig P, Engel AK, Singer W. Oscillatory responses in cat visual cortex exhibit inter-columnar synchronization which reflects global stimulus properties. Nature 1989;338(6213):334–7.
Happe F, Frith U. The weak coherence account: detail-focused cognitive style in autism spectrum disorders. J Autism Dev Disord 2006;36(1):5–25.

Herbert MR, Ziegler DA, Deutsch CK, O'Brien LM, Lange N, Bakardjiev A, et al. Dissociations of cerebral cortex, subcortical and cerebral white matter volumes in autistic boys. Brain 2003;126(Pt 5):1182–92.

Herbert MR, Ziegler DA, Makris N, Filipek PA, Kemper TL, Normandin JJ, et al. Localization of white matter volume increase in autism and developmental language disorder. Ann Neurol 2004;55(4):530–40.

Just MA, Cherkassky VL, Keller TA, Kana RK, Minshew NJ. Functional and anatomical cortical underconnectivity in autism: evidence from an FMRI study of an executive function task and corpus callosum morphometry. Cereb Cortex 2007;17(4):951–61.

Just MA, Cherkassky VL, Keller TA, Minshew NJ. Cortical activation and synchronization during sentence comprehension in high-functioning autism: evidence of underconnectivity. Brain 2004;127(Pt 8):1811–21.

Lakatos P, Karmos G, Mehta AD, Ulbert I, Schroeder CE. Entrainment of neuronal oscillations as a mechanism of attentional selection. Science 2008;320(5872):110–3.

Lazarev VV, Pontes A, deAzevedo LC. EEG photic driving: right-hemisphere reactivity deficit in childhood autism. A pilot study. Int J Psychophysiol 2009;71(2):177–83.

Lazarev VV, Pontes A, Mitrofanov AA, Deazevedo LC. Interhemispheric asymmetry in EEG photic driving coherence in childhood autism. Clin Neurophysiol 2010;121(2):145–52.

Lord C, Risi S, Lambrecht L, Cook Jr EH, Leventhal BL, DiLavore PC, et al. The autism diagnostic observation schedule-generic: a standard measure of social and communication deficits associated with the spectrum of autism. J Autism Dev Disord 2000;30(3):205–23.

Lord C, Rutter M, Le Couteur A. Autism diagnostic interview-revised: a revised version of a diagnostic interview for caregivers of individuals with possible pervasive developmental disorders. J Autism Dev Disord 1994;24(5):659–85.

Milne E, Scope A, Pascalis O, Buckley D, Makeig S. Independent component analysis reveals atypical electroencephalographic activity during visual perception in individuals with autism. Biol Psychiatry 2009;65(1):22–30.

Mima T, Oluwatimilehin T, Hiraoka T, Hallett M. Transient interhemispheric neuronal synchrony correlates with object recognition. J Neurosci 2001;21(11):3942–8.

Mizuno A, Villalobos ME, Davies MM, Dahl BC, Muller RA. Partially enhanced thalamocortical functional connectivity in autism. Brain Res 2006;1104(1):160–74.

Mottron L, Dawson M, Soulieres I. Enhanced perception in savant syndrome: patterns, structure and creativity. Philos Trans R Soc London B Biol Sci 2009;364(1522):1385–91.

Murias M, Webb SJ, Greenson J, Dawson G. Resting state cortical connectivity reflected in EEG coherence in individuals with autism. Biol Psychiatry 2007;62(3):270–3.

Nikouline VV, Linkenkaer-Hansen K, Huttunen J, Ilmoniemi RJ. Interhemispheric phase synchrony and amplitude correlation of spontaneous beta oscillations in human subjects: a magnetoencephalographic study. Neuroreport 2001;12(11):2487–91.

Nolte G, Bai O, Wheaton L, Mari Z, Vorbach S, Hallett M. Identifying true brain interaction from EEG data using the imaginary part of coherency. Clin Neurophysiol 2004;115(10):2292–307.

Nunez PL, Srinivasan R, Westdorp AF, Wijesinghe RS, Tucker DM, Silberstein RB, et al. EEG coherency. I: Statistics, reference electrode, volume conduction, Laplacians, cortical imaging, and interpretation at multiple scales. Electroen Clin Neurophysiol 1997;103(5):499–515.

Orekhova EV, Stroganova TA, Nygren G, Tsetlin MM, Posikera IN, Gillberg C, et al. Excess of high frequency electroencephalogram oscillations in boys with autism. Biol Psychiatry 2007;62(9):1022–9.

Ozerdem A, Guntekin B, Tunca Z, Basar E. Brain oscillatory responses in patients with bipolar disorder manic episode before and after valproate treatment. Brain Res 2008;1235:98–108.

Pardo CA, Eberhart CG. The neurobiology of autism. Brain Pathol 2007;17(4):434–47.

Pearson Education, I. BASC-2: behavior assessment system for children, 2nd ed.; 2008.

Pfurtscheller G, Flotzinger D, Neuper C. Differentiation between finger, toe and tongue movement in man based on 40 Hz EEG. Electroen Clin Neurophysiol 1994;90(6):456–60.

Rodriguez E, George N, Lachaux JP, Martinerie J, Renault B, Varela FJ. Perception's shadow: long-distance synchronization of human brain activity. Nature 1999;397(6718):430–3.

Sederberg PB, Kahana MJ, Howard MW, Donner EJ, Madsen JR. Theta and gamma oscillations during encoding predict subsequent recall. J Neurosci 2003;23(34):10809–14.

Sporns O, Tononi G, Edelman GM. Theoretical neuroanatomy: relating anatomical and functional connectivity in graphs and cortical connection matrices. Cereb Cortex 2000;10(2):127–41.

Tallon-Baudry C, Bertrand O, Delpuech C, Pernier J. Stimulus specificity of phase-locked and non-phase-locked 40 Hz visual responses in human. J Neurosci 1996;16(13):4240–9.

Torrence C, Compo GP. A practical guide to wavelet analysis. Bull Am Meteorol Soc 1998;79:61–78.

Varela F, Lachaux JP, Rodriguez E, Martinerie J. The brainweb: phase synchronization and large-scale integration. Nat Rev 2001;2(4):229–39.

Villalobos ME, Mizuno A, Dahl BC, Kemmotsu N, Muller RA. Reduced functional connectivity between V1 and inferior frontal cortex associated with visuomotor performance in autism. NeuroImage 2005;25(3):916–25.

von Stein A, Chiang C, Konig P. Top-down processing mediated by interareal synchronization. Proc Natl Acad Sci USA 2000;97(26):14748–53.

Yuval-Greenberg S, Tomer O, Keren AS, Nelken I, Deouell LY. Transient induced gamma-band response in EEG as a manifestation of miniature saccades. Neuron 2008;58(3):429–41.